Brain Advance Access published March 20, 2015

doi:10.1093/brain/awv051 BRAIN 2015: Page 1 of 12 | 1

BRAIN
A JOURNAL OF NEUROLOGY

Autism: reduced connectivity between cortical areas involved in face expression, theory of mind, and the sense of self

Wei Cheng,[1,*] Edmund T. Rolls,[2,3,*] Huaguang Gu,[4,*] Jie Zhang[1] and Jianfeng Feng[1,2]

*These authors contributed equally to this work.

Whole-brain voxel-based unbiased resting state functional connectivity was analysed in 418 subjects with autism and 509 matched typically developing individuals. We identified a key system in the middle temporal gyrus/superior temporal sulcus region that has reduced cortical functional connectivity (and increased with the medial thalamus), which is implicated in face expression processing involved in social behaviour. This system has reduced functional connectivity with the ventromedial prefrontal cortex, which is implicated in emotion and social communication. The middle temporal gyrus system is also implicated in theory of mind processing. We also identified in autism a second key system in the precuneus/superior parietal lobule region with reduced functional connectivity, which is implicated in spatial functions including of oneself, and of the spatial environment. It is proposed that these two types of functionality, face expression-related, and of one's self and the environment, are important components of the computations involved in theory of mind, whether of oneself or of others, and that reduced connectivity within and between these regions may make a major contribution to the symptoms of autism.

1 Centre for Computational Systems Biology, Fudan University, Shanghai, PR China
2 Department of Computer Science, University of Warwick, Coventry CV4 7AL, UK
3 Oxford Centre for Computational Neuroscience, Oxford, UK
4 School of Aerospace Engineering and Applied Mechanics, Tongji University, Shanghai 200092, PR China

Correspondence to: Professor Jianfeng Feng,
Department of Computer Science,
University of Warwick,
Coventry CV4 7AL,
UK
E-mail: Jianfeng.Feng@warwick.ac.uk

Keywords: Autistic spectrum disorder; behavioural neurology; neuropsychiatry imaging social cognition; temporal lobe

Abbreviations: AAL = Automated Anatomical Labelling; ADOS = Autism Diagnostic Observational Schedule; ITG = inferior temporal gyrus; MFG = middle frontal gyrus; MTG = middle temporal gyrus; ORBsupmed = ventromedial prefrontal cortex; PoCG = post-central gyrus; STG = superior temporal gyrus; STS = superior temporal sulcus

Introduction

Autism spectrum disorder is a complex developmental disorder that is characterized by difficulties in social communication and social interaction; and restricted and repetitive behaviour, interests or activities (Lai *et al.*, 2014). Recently, a great deal of attention has been focused on the delineation of neural systems for brain–behaviour relationships in autism spectrum disorder given that ~1% of children are being diagnosed with this disorder (Kim *et al.*, 2011).

Received June 10, 2014. Revised January 2, 2015. Accepted January 4, 2015.

At the brain circuit level, most of what we understand about autism and its biological abnormalities during the resting state comes from functional MRI studies targeting changes in a small number of brain regions, as recently reviewed (Minshew and Keller, 2010; Müller *et al.*, 2011; Maximo *et al.*, 2014). These studies have suggested abnormality in connectivity between a group of related and partly overlapping brain systems characterized as the default mode network (Assaf *et al.*, 2010; Lynch *et al.*, 2013), social brain circuits (Gotts *et al.*, 2012; Kennedy and Adolphs, 2012), self-representation circuitry (Lombardo *et al.*, 2010), reward circuitry (Dichter *et al.*, 2012*a*, *b*), the salience network (Uddin *et al.*, 2013), a motor control network (Kenet *et al.*, 2012), and an imitation network (Shih *et al.*, 2010). Despite the large and growing body of reports of abnormal functional connectivity in autism, inconsistencies in findings remain regarding the altered pattern of connectivity and the localization of the brain areas involved. This may be attributed to individual site-specific studies with relatively small sample sizes, coupled with the analysis performed.

The conclusions drawn from these studies are from either seed-based analysis, independent component analysis (ICA), or parcellation-based analysis [using for example the 90 regions in the Automated Anatomical Labelling (AAL) template (Tzourio-Mazoyer *et al.*, 2002)] and these have some limitations. Seed-based analysis is a hypothesis-driven approach, which means the foci (seeds) of the disorder must be specified *a priori*. It is therefore a biased approach lacking a global and independent view. With the ICA approach it is assumed that the human brain is composed of independent components, whereas different parts of the human brain work in a coordinated fashion. Moreover, ICA-based approaches typically only characterize differences in correlations between specific voxels' time series and a network-wide time series, rather than correlations between signals from specific regions. Parcellation-based whole brain analysis also is not fully unbiased due to the choice of the parcellation scheme, which directly specifies the nodes (regions) and edges (connections) of a macroscopic brain network (de Reus and Van den Heuvel, 2013). Hence, given the complexity and multiple causes of autism together with variability between individuals, a novel, unbiased approach is urgently called for which identifies pathway changes in a whole-brain voxel-based manner and Gotts *et al.* (2012) have described a voxel-wise whole brain comparison of functional connectivity differences between autism and controls.

In the current paper, we describe the first voxel-level pairwise whole brain comparison of resting state functional connectivity differences between subjects with autism and controls. For this we needed a large number of autistic people and controls, and were able to use for this analysis data in a large resting state functional MRI data set, the autism brain imaging data exchange (ABIDE; http://fcon_1000.projects.nitrc.org/indi/abide/), which has already proved useful (Di Martino *et al.*, 2014). The pair-wise voxel-level analysis presented here goes beyond previous studies because it assesses, across the whole brain, which pairs of voxels have different functional connectivity between subjects with autism and controls.

Materials and methods

Overall design

We analysed resting state functional MRI data from 418 autistic subjects and 509 controls to achieve sufficient statistical power for this first voxel-pair based whole brain comparison of resting state functional connectivity differences. A flow chart of the brain-wide association study [termed BWAS, in line with genome-wide association studies (GWAS)] is shown in Fig. 1. This 'discovery' approach tests for differences between patients and controls in the connectivity of every pair of brain voxels at a whole-brain level. Unlike previous seed-based or independent components-based approaches, this method has the advantage of being fully unbiased, in that the connectivity of all brain voxels can be compared, not just selected brain regions. Additionally, we investigated clinical associations between the identified abnormal circuitry and symptom severity; and we also investigated the extent to which the analysis can reliably discriminate between patients and controls using a pattern classification approach. Further, we confirmed that our findings were robust by split data cross-validations.

Participants

The ABIDE repository is hosted by the 1000 Functional Connectome Project/International Neuroimaging Data-sharing Initiative (INDI) (see http://fcon_1000.projects.nitrc.org for more information and other data sets), and consists of 1112 data sets comprised of 539 autism and 573 typically developing individuals. All data are fully anonymized in accordance with HIPAA (Health Insurance Portability and Accountability) guidelines, and research procedures and ethical guidelines were followed in accordance with the Institutional Review Boards (IRB) of the respective participating institution. All data released were visually inspected by members of the ABIDE project. Details of diagnostic criteria, acquisition, informed consent, and site-specific protocols are available at: http://fcon_1000.projects.nitrc.org/indi/abide/. The inclusion criteria for sample selection included: (i) functional MRI data were successfully preprocessed with manual visual inspection of normalization to MNI space; (ii) any data with a mean framewise displacement exceeding 0.2 mm were excluded; (iii) subjects were excluded if the percentage of 'bad' points (framewise displacement >0.5 mm) was over 25% in volume censoring (scrubbing, see below); (iv) subjects with a full IQ exceeding 2 standard deviations (SD) from the overall ABIDE sample mean (108 ± 15) were not included; and (v) data collection centres were only included in our analysis if they had at least 20 participants after the above exclusions. A total of 927 subjects met all inclusion criteria (418 subjects with autism and 509 otherwise matched typically developing subjects from 16 centres). The demographic and clinical characteristics of participants satisfying the inclusion criteria are summarized in Supplementary Table 1.

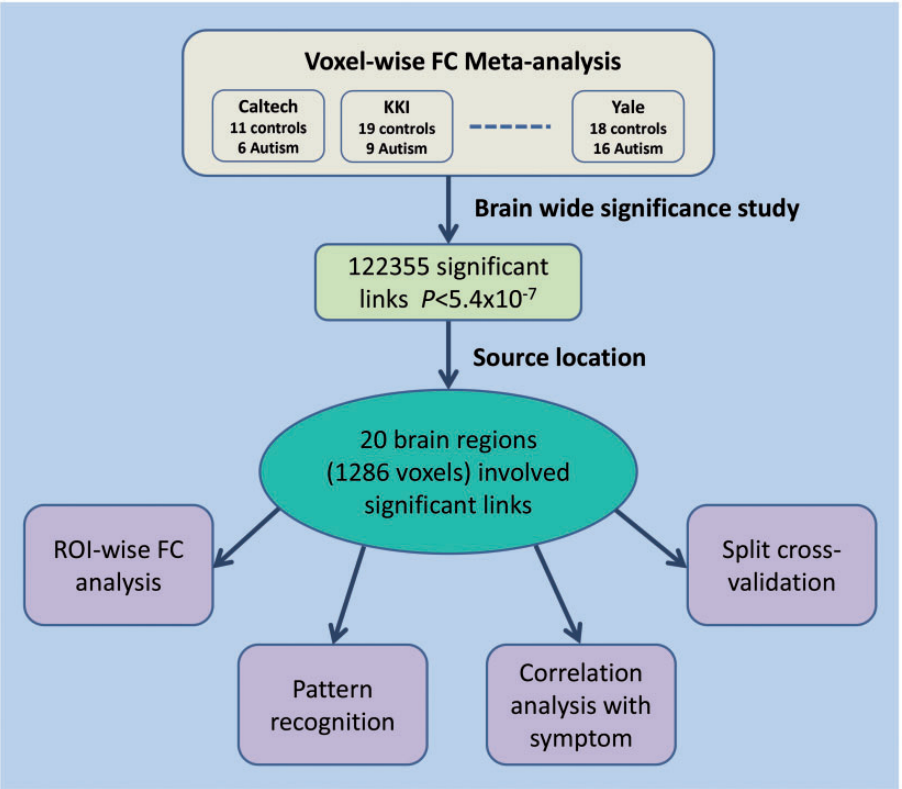

Figure 1 Flow chart of the voxel-wise functional connectivity meta-analysis on the autism data set. FC = functional connectivity; ROI = region of interest.

Image acquisition and preprocessing

In the ABIDE initiative, pre-existing data are shared, with all data being collected at a number of different centres with 3 T scanners. Details regarding data acquisition for each sample are provided on the ABIDE website (http://fcon_1000.projects.nitrc.org/indi/abide).

Preprocessing and statistical analysis of functional images were carried out using the Statistical Parametric Mapping package (SPM8, Wellcome Department for Imaging Neuroscience, London, UK). For each individual participant's data set, the first 10 image volumes were discarded to allow the functional MRI signal to reach a steady state. Initial analysis included slice time correction and Motion realignment. The resulting images were then spatially normalized to the Montreal Neurological Institute (MNI) EPI template in SPM8, resampled to $3 \times 3 \times 3\,mm^3$, and subsequently smoothed with an isotropic Gaussian kernel (full-width at half-maximum = 8 mm).

To remove possible sources of spurious correlations present in resting-state blood oxygenation level-dependent data, all functional MRI time-series underwent high-pass temporal filtering (0.01 Hz), nuisance signal removal from the ventricles and deep white matter, global mean signal removal, and motion correction with six rigid-body parameters, followed by low-pass temporal filtering (0.08 Hz). In addition, given views that excessive movement can impact between-group differences, we used four procedures to achieve motion correction. In the first step, we carried out 3D motion correction by aligning each functional volume to the mean image of all volumes. In the second step, we implemented additional careful volume censoring ('scrubbing') movement correction (Power *et al.*, 2014) to ensure that head-motion artefacts were not driving observed effects. The mean framewise displacement was computed with the framewise displacement threshold for exclusion being a displacement of 0.5 mm. In addition to the frame corresponding to the displaced time point, one preceding and two succeeding time points were also deleted to reduce the 'spill-over' effect of head movements. Thirdly, subjects with >25% displaced frames flagged or mean framewise displacement exceeding 0.2 mm were completely excluded from the analysis as it is likely that this level of movement would have had an influence on several volumes. Finally, we used the mean framewise displacement as a covariate when comparing the two groups during statistical analysis.

Voxel-level association study

In the present study, each resting state functional MRI image included 47 636 voxels. For each pair of voxels in this whole brain pair-wise voxel-level analysis, the time series were extracted and their correlation was calculated for each subject followed by *z*-transformation and two-tailed, two-sample *t*-tests were performed on the 1 134 570 430 (47 636 × 47 635 / 2) Fisher's *z*-transformed correlation coefficients to identify significantly altered functional links in autism patients compared to controls within each imaging centre. The Liptak-Stouffer *z*-score method (Liptak, 1958) was then used to combine the results from the

individual data sets, weighted by sample size, after removing the variance explained by differences in age, gender ratios, handedness, and full IQ. To avoid possible head motion artefacts, the mean framewise displacements were regressed again in the meta-analysis. This can be described as a meta-analytic approach performed across data sets from different imaging centres at the individual voxel-level across the whole brain to more precisely identify the localization of altered functional connectivity that typifies autism. A false discovery rate (FDR) procedure was used to correct for multiple comparisons. A measure for the association (*MA*) between a voxel i and the brain disorder was then defined as: $MA(i) = N_\alpha$, where N_α is the number of links between voxel i and every other voxel in the brain that have a P-value $< \alpha$ (which in the present study with FDR correction was $P < 0.005$), corresponding to a P-threshold of 5.4×10^{-7} in t-tests. A larger value of *MA* implies a more significant alteration in functional connectivity. To control the false positive rate, we used a relatively strict threshold (FDR $P < 0.005$) and set two other thresholds, on *MA* (>40), and on voxel cluster size (>30), when assessing which voxels had the significant differences between the two groups (as will be shown in Fig. 2).

The measure of association (*MA*) value described above shows voxels with significantly different functional connectivities, but not the brain regions to which these voxels have altered connectivity. To facilitate the explanation of our results, we also show the pattern of the altered connectivity in the 'Results' section.

Correlations with symptom severity

We used the kernel generalized variance (S1) (Bach and Jordan, 2003) to quantify the dependency between differences in functional connectivity and social symptom severity in autism spectrum disorder as assessed by the Autism Diagnostic Observational Schedule (ADOS) total, communication, social and stereotyped behaviour scores. The kernel generalized variance gives an estimate of the mutual information between two sets of variables (e.g. functional connectivities and ADOS scores), is exact when the variables are jointly Gaussian, and is an approximation to the second order when the variables in question are from arbitrary distributions and 'nearly independent' (Bach and Jordan, 2003). Statistical inference was based on a permutation procedure.

Pattern classification based on the altered functional connectivity

To further test the clinical relevance of the main identified autism links as diagnostic features of autism, we applied a support vector machine (SVM) approach using the alterations in the regions of interest as a biomarker to test how well this could discriminate patients with autistic spectrum disorder from the healthy controls, that is, classify individuals into one of these groups. In particular, features were first extracted from the voxel-based region of interest-wise functional connectivities ($20 \times 19 / 2 = 190$ correlation coefficients) exhibiting significant group differences examined by two-sample t-test. We used a leave-one-out cross-validation strategy to estimate the generalization of this classifier and to estimate its accuracy, sensitivity and specificity.

Robustness analysis

To test for robustness of the significant regions identified by the previous analyses using the whole data set, we performed a half-split reliability analysis in the time domain. In other words, for each subject, we split the full-time functional MRI signals into two equal time series, the first half and the second half (Gotts *et al.*, 2012). *MA* was recalculated and then analysed separately for both data sets with identical methods. Then one of the splits was used to define regions of interest, while the other split was used for cross-validation, including region of interest-wise functional connectivity analyses and classifications.

Results

Whole-brain voxel-based functional networks

Figure 2B (and Supplementary Fig. 1 with coronal slices) shows the locations of all voxels in the brain that had significantly different functional connectivities between the autistic and the control populations. These voxels had some functional connectivities that were significantly different across the whole brain after FDR correction; with the FDR $P < 0.005$, the significance level uncorrected had to be $P < 5.4 \times 10^{-7}$. In fact, many of the functional connectivities had $P < 10^{-10}$, and this was only possible with the large numbers of subjects in the investigation. In fact, similar results with Bonferroni correction ($P < 4.4 \times 10^{-11}$) are also obtained and are shown in Supplementary Fig. 2. Voxels that had functional connectivities in the autism population that were larger than in controls are shown in red, with the measure of association reflecting the number of significantly different links a particular voxel had. Voxels that had functional connectivities in the autism population that were weaker than in controls are shown in blue. Several main groups of voxels are evident in Fig. 2B, in the superior, middle and inferior temporal gyrus; pre- and post-central gyrus; superior frontal gyrus (dorsolateral); middle frontal gyrus; supplementary motor area; ventromedial prefrontal cortex (ORBsupmed); cuneus, precuneus, and paracentral lobule; caudate nucleus; and thalamus. These voxel-based data are shown in coronal slices of the brain in Supplementary Fig. 1.

To help define the locations of these significant voxels and further analyse the connectivities, the voxels were categorized into regions of interest defined by the 90 areas of the AAL atlas (see Supplementary Table 2 for a list of abbreviations and the corresponding numbers). Figure 2A shows for each AAL region the P-values for each voxel in each AAL region with a functional connectivity link to any of the other 47 635 voxels in the brain that was significantly different ($P < 10^{-5}$) between the two populations. Figure 2A shows that there were many functional connectivity links that were significant after FDR correction. The 20 AAL regions that contained 20 or more

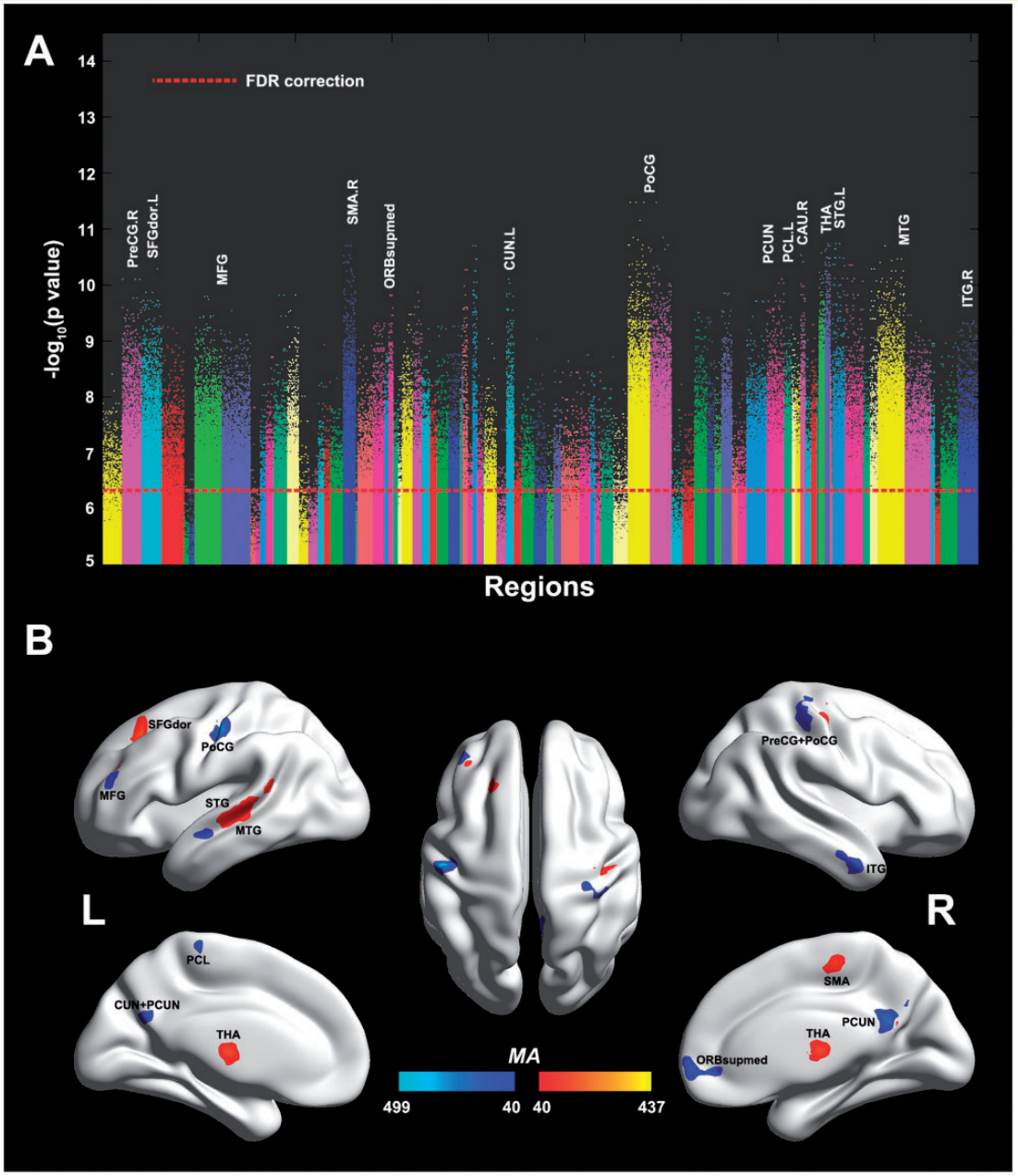

Figure 2 Voxels with different functional connectivity in autism. (**A**) Manhattan plot showing the probability values for each link being different in the autistic group compared to the control group. Each dot is a functional connectivity link between two voxels. Note there are a total of 47 636 × 47 635 / 2 links, and we only plot a dot if $P < 10^{-5}$. The red dotted line is the FDR correction threshold $P = 5.4 \times 10^{-7}$. The regions indicate the AAL areas in which the voxels were located, with the numbers for each region specified in Supplementary Table 2. (**B**) Location of the voxels that had significantly different altered functional connectivity with other voxels (using whole brain FDR correction). The colour bar represents the measure of association (*MA*, see text) given by the number of significantly affected links relating to each voxel. Voxels that had functional connectivities in the autism population that were weaker (# weak links > # strengthened links) than in controls are shown in blue, and that had stronger functional connectivity in the autism population are shown in red. Six main groups of voxels are evident, in the MTG, ventromedial prefrontal cortex (ORBsupmed), precuneus (PCUN) and paracentral lobule (PCL), the post- and precentral gyri (PoCG and PreCG), and a medial region of the thalamus (THA). SFGdors=superior frontal gyrus, dorsal part.

significant voxels are named in Fig. 2A. The coordinates of the regions of interest of 20 or more voxels are shown in Table 1.

One main cluster of voxels was in the left middle temporal gyrus (MTG) [−57 −24 0] [region of interest (ROI) 18], with also a cluster in the right MTG (ROI 19) and right inferior temporal gyrus (ITG) (ROI 20) (Table 1). The coordinates of the posteroventral part of the voxels in the left MTG area were [−56 −37 2], and this has been identified as an area with activations related to face expression,

Table 1 Significant regions of interest in the voxel-based whole brain analysis

No.	Areas	# Voxels in ROI	Peak *MA* value	MNI coordinates (Peak)
ROI 1	Right precentral gyrus	49	117	36 −21 54
ROI 2	Left superior frontal gyrus, dorsolateral	37	340	−21 27 45
ROI 3	Left MFG	69	182	−39 45 24
ROI 4	Right MFG	23	−371	51 48 3
ROI 5	Right supplementary motor area	34	135	9 −21 54
ROI 6	Left ventromedial prefrontal cortex	20	−155	0 63 −6
ROI 7	Right ventromedial prefrontal cortex	68	−250	3 63 −6
ROI 8	Left cuneus	22	−114	−6 −63 27
ROI 9	Left postcentral gyrus	110	−449	−51 −15 48
ROI 10	Right postcentral gyrus	145	−152	33 −27 54
ROI 11	Left precuneus	44	−95	−3 −66 30
ROI 12	Right precuneus	47	−210	6 −51 24
ROI 13	Left paracentral lobule	30	−112	−12 −36 72
ROI 14	Right caudate nucleus	32	424	15 −6 18
ROI 15	Left thalamus	145	352	−9 −15 12
ROI 16	Right thalamus	146	437	15 −9 18
ROI 17	Left STG	29	133	−57 −45 18
ROI 18	Left MTG	178	160	−57 −24 0
ROI 19	Right MTG	25	−308	60 0 −30
ROI 20	Right ITG	33	−294	57 0 −30

A region of interest (ROI) was defined as an area in an AAL region with $\geqslant$20 significant voxels after Bonferroni correction. The measure of association (*MA*) is shown as positive if overall the voxel has stronger functional connectivity links in subjects with autism, and as negative if they are weaker.

with this and the more anterior part of this cluster implicated in theory of mind processing (see 'Discussion' section); ROI 17 is a small further group of voxels in the temporal cortex. A second cluster was in the medial thalamus (left thalamus [−9 −15 12], right thalamus [15 −9 18]) (see Table 1 and Supplementary Fig. 1). A third cluster was in the post-central cortex in the face somatosensory area (PoCG, ROIs 9 and 10). A fourth cluster was in the ventromedial prefrontal cortex (ORBsupmed, ROIs 6 and 7) (in or close to cytoarchitectonic area 32 cingulate cortex / 10 medial prefrontal cortex / 11 medial orbitofrontal cortex), a region implicated in emotion (Rolls, 2014, 2015). A fifth cluster was in the middle frontal gyrus (MFG) (left MFG [−39 45 24], right MFG [51 48 3]) (Table 1, Fig. 2B and Supplementary Fig. 1). A sixth cluster was in the right precuneus [6 −51 24] (right precuneus ROI 12), with a corresponding cluster in the left hemisphere. This is part of medial parietal cortex area 7. A seventh cluster was in the paracentral lobule (left paracentral lobule ROI 13), which is part of superior parietal cortex area 7 with connections to the precuneus (Margulies *et al.*, 2009).

Altered functional connectivity pattern

To investigate the abnormal connectivity pattern in the functional connectivity networks in autism, all significant voxels (after FDR correction) were parcellated into regions according to the AAL atlas (Tzourio-Mazoyer *et al.*, 2002). On this basis, 20 regions of interest were identified in which there were 20 or more significant voxels, as shown in Table 1 and Fig. 2B. The time series were extracted in each region of interest by averaging the blood oxygenation level-dependent signals of all significant voxels within that region. The functional connectivity was evaluated between each pair of regions of interest using a Pearson correlation coefficient. Then region of interest-wise functional connectivity analysis on the significant voxels within each region of interest was performed to compare patient groups and their respective healthy controls. Finally, we obtained a 20 × 20 symmetric matrix (in Fig. 3A, which only shows links with Bonferroni correction with a threshold of $P < 2.6 \times 10^{-4}$) that shows the overall pattern of the different connectivity patterns between these voxel clusters in the autistic group compared to the control group.

Based on the effects measured using the 20 or more significant voxels in each AAL region, the findings in Fig. 3 may be summarized as follows: there was increased functional connectivity in the autistic group between the medial thalamus and the left MTG and superior temporal gyrus (STG); and between the medial thalamus and the post-central gyrus (somatosensory cortex). Most cortico-cortical links that showed a significant change had a decrease in functional connectivity in subjects with autism. These included links of the MTG (right MTG and right ITG) with the ventromedial prefrontal cortex (ORBsupmed), left superior frontal gyrus, precuneus and cuneus. Decreased functional connectivity was found between the precuneus and cuneus, MTG, and ventromedial prefrontal cortex (ORBsupmed). The post-central gyrus had decreased

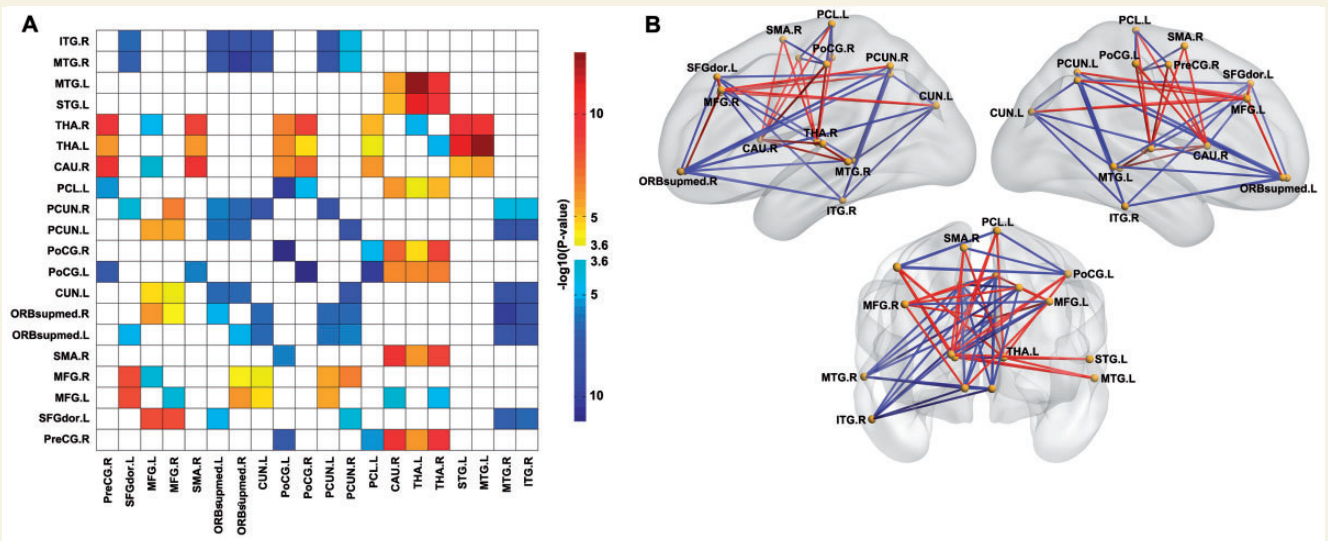

Figure 3 The pattern of altered functional connectivity. (**A**) The functional connectivity matrix calculated from the blood oxygenation level-dependent signals in the significant voxels in each of the 20 regions of interest based on the 20 AAL regions that contained $\geqslant 20$ significant voxels. Probability values are shown in the chart as red if they are significantly stronger in the autistic group, and blue if they are significantly weaker in the autistic group, after Bonferroni correction (see colour bar for *P*-values). (**B**) A schematic diagram showing the voxel region of interest-based connectivity differences between the autistic and the control group. The glass brains were generated using BrainNet Viewer (http://www.nitrc.org/projects/bnv/). CAU = caudate; CUN = cuneus; PCL = paracentral lobule; PCUN = precuneus; PreCG = precentral gyrus; SFGdor = superior frontal gyrus; SMA = supplementary motor area.

connectivity in the autism group with the paracentral lobule. Figure 3B provides a schematic brain-based diagram of these altered functional connectivities based on the significant voxels in the 20 regions of interest. The altered patterns of functional connections were consistent across the data sets from the 16 different imaging centres (Supplementary Fig. 7). Significant differences between the populations in the voxel-wise functional connectivity pattern are shown schematically in Supplementary Fig. 8.

Correlations of the altered functional connectivity links with the autism scores

The kernel generalized variance was used to give an estimate of the correlation between the two sets of variables, namely the altered functional connectivities ($20 \times 19 / 2 = 190$ links) and the four ADOS symptom severity scores. This test showed that the functional connectivity changes were significantly associated with the symptom severity scores ($P < 0.04$). On this basis, we performed a *post hoc* analysis to investigate whether differences in individual functional connectivity links were correlated with the symptoms of autism. In a *post hoc* illustrative analysis, we calculated the partial correlation between the strength of the functional connectivities between the significant voxels in the 20 region of interest AAL-based areas, and the ADOS subscores removing the variance explained by differences in age and sex. As can be seen from Table 2, there were significant correlations ($P < 0.05$) between some of the region of interest-wise functional links and the symptom severity scores. A negative correlation (R) in Table 2 indicates that the weakening of a connectivity link is associated with the severity of a symptom. Of particular interest is that the ADOS communication score was correlated with weakened connectivity of the MTG with the superior frontal gyrus, precuneus and paracentral lobule; and between the cuneus and precuneus. Also of interest is that the ADOS social score was correlated with weakened connectivity between the temporal gyrus (MTG or ITG or STG) and the paracentral lobule and precuneus; and of the orbitofrontal/cingulate cortex (ORBsupmed) with the middle frontal gyrus and caudate nucleus.

Classification of autism based on the altered functional connectivity links in autism

To further test the functional significance of the links identified as related to autism, we used a support vector machine analysis to investigate the utility of the altered network as a biomarker for discriminating autistic subjects from controls. Figure 4 shows that the highest discrimination power is achieved in the Oregon Health and Science University (OHSU) data set (sample size = 26), with an accuracy of 96% for distinguishing autistic subjects from controls; and that the accuracy from the data from most imaging centres reached 80%. Permutation tests revealed that within and across data sets, discrimination accuracies were highly significant ($P < 0.01$ in most cases). These results are summarized in Supplementary Table 3.

Table 2 Correlations between the functional connectivity links and the autism symptom severity scores

Links		ADOS_TOTAL		ADOS_COMM		ADOS_SOCIAL		ADOS_STEREO_BEHAV	
		R	P	R	P	R	P	R	P
PreCG.R	ORBsupmed.L	0.1226	**0.0322**	0.1186	**0.0489**	0.0947	0.0972	−0.0893	0.2489
PreCG.R	PoCG.R	−0.1477	**0.0137**	−0.0837	0.1855	−0.1408	**0.0267**	−0.1061	0.1179
SFGdor.L	PoCG.L	−0.0704	0.2890	−0.1279	**0.0435**	−0.0778	0.2866	−0.0031	0.9855
SFGdor.L	PoCG.R	−0.1120	0.0660	−0.1493	**0.0177**	−0.0969	0.1370	−0.0657	0.3679
SFGdor.L	MTG.R	−0.0696	0.2210	−0.1231	**0.0290**	−0.0530	0.3886	−0.0550	0.4778
MFG.L	SMA.R	0.1095	0.0725	0.1354	**0.0318**	0.0670	0.3021	0.0523	0.4996
MFG.L	ORBsupmed.R	0.1169	**0.0416**	−0.0021	0.9736	0.1112	**0.0495**	−0.0396	0.6520
MFG.L	PCL.L	0.1203	**0.0467**	0.1317	**0.0367**	0.0824	0.1878	0.0726	0.3486
MFG.L	CAU.R	−0.1302	**0.0289**	−0.1059	0.0794	−0.0871	0.1725	−0.0346	0.6101
MFG.R	PoCG.L	−0.0088	0.8802	0.0366	0.5512	−0.0030	0.9412	0.2048	**0.0047**
SMA.R	PoCG.L	−0.1289	**0.0327**	−0.1890	**0.0010**	−0.0698	0.2830	−0.0185	0.7873
SMA.R	MTG.L	−0.1312	**0.0231**	−0.1097	0.0638	−0.1228	0.0573	−0.1173	0.1048
ORBsupmed.L	CAU.R	0.1059	0.0796	0.0131	0.8377	0.1306	**0.0425**	0.0375	0.6667
CUN.L	PCUN.L	−0.0464	0.4675	−0.1297	**0.0416**	0.0254	0.6696	0.0807	0.2347
CUN.L	PCUN.R	−0.0651	0.2959	−0.1353	**0.0335**	−0.0385	0.5566	0.0143	0.8172
PoCG.L	PoCG.R	−0.1771	**0.0034**	−0.1508	**0.0158**	−0.1349	**0.0347**	−0.0836	0.2432
PoCG.L	PCL.L	−0.1308	**0.0242**	−0.1638	**0.0041**	−0.1019	0.1107	−0.0884	0.2310
PoCG.R	STG.L	−0.1258	**0.0421**	−0.0717	0.2483	−0.1427	**0.0288**	−0.0954	0.2016
PCUN.R	MTG.L	0.1434	**0.0169**	0.1561	**0.0118**	0.1495	**0.0173**	0.1077	0.1569
PCL.L	STG.L	−0.1131	**0.0464**	−0.0761	0.2034	−0.1200	**0.0425**	−0.0606	0.4313
PCL.L	MTG.L	−0.1456	**0.0120**	−0.1215	**0.0492**	−0.1292	**0.0322**	−0.0198	0.8011
STG.L	MTG.R	0.0711	0.2314	0.0431	0.4374	0.1254	**0.0429**	0.0060	0.9233
STG.L	ITG.R	0.0801	0.1738	0.0722	0.2014	0.1276	**0.0390**	0.0711	0.3179
MTG.L	MTG.R	0.0823	0.1315	0.0438	0.3935	0.1302	**0.0270**	0.0998	0.1764
MTG.L	ITG.R	0.1104	0.0582	0.0888	0.1221	0.1553	**0.0119**	0.1737	**0.0172**

ADOS_COMM = ADOS communication score; ADOS_STEREO_BEHAV = ADOS stereotyped behaviour score; ADOS_SOCIAL = ADOS social score; ADOS_TOTAL = ADOS total score; CAU = caudate; CUN = cuneus; PCL = paracentral lobule; PCUN = precuneus; PreCG = precentral gyrus; SFGdor = superior frontal gyrus; SMA = supplementary motor area; L = left; R = right. The functional connectivity measure was that between the blood oxygenation level-dependent signals in the significant voxels in the two AAL regions specified.

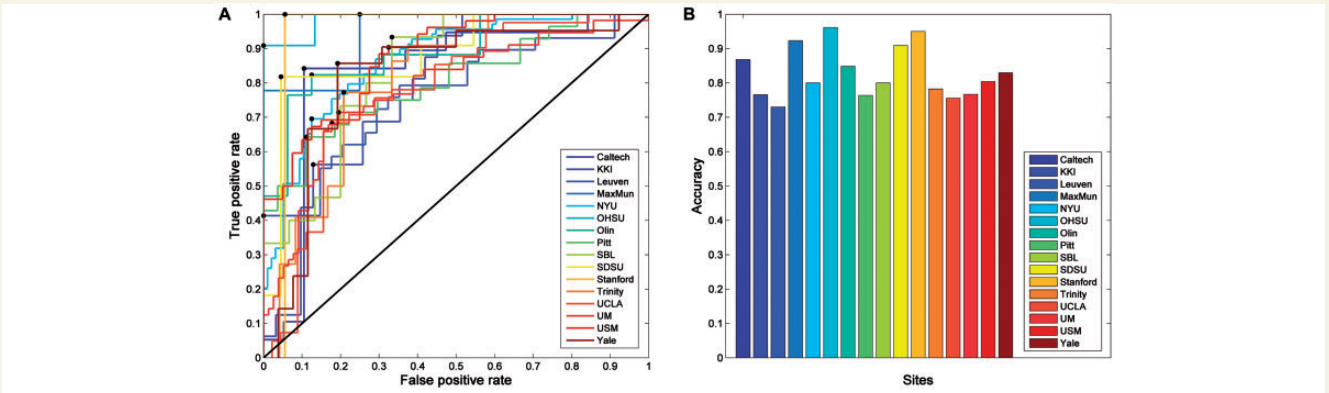

Figure 4 Classification of individuals as autistic versus controls using the voxel-based region of interest-wise functional connectivity measures identified. (**A**) Receiver operating characteristic (ROC) curves showing the true positive rate plotted against the false positive rate are provided for each of the centres that contributed subjects to the database. (**B**) Accuracy (percentage correct) classification of a subject as autistic or in the control group for the data from each of the centres.

The robustness of the results

Supplementary Fig. 3 shows the locations of all voxels in the brain that have significantly different functional connectivities between the autistic and the control population for both data sets (FDR correction, 0.05, *MA* >40, cluster size >30 voxels). We highlight in Supplementary Fig. 3 regions that exhibit differences in all three cases: the whole data set, the first half, and the second half. We found that the most significant regions were consistent across these three cases.

In our analyses, all significant voxels (after FDR correction $P < 0.05$) were parcellated into regions according to the AAL atlas. For the first half data set, 45 regions of interest were identified in which there were $\geqslant 20$ significant voxels, as shown in Supplementary Table 4. For the second half data set, 36 regions of interest were identified in which there were $\geqslant 20$ or more significant voxels, as shown in Supplementary Table 4. More than 90% identical regions (except left cuneus and paracentral lobule) were significant in all three cases: the whole data set, the first half, and the second half (Tables 1 and Supplementary Table 4). One of the splits was then used to define regions of interest as described above, while the other split was used for cross-validation, including region of interest-wise functional connectivity analyses and classifications. The robustness of the results obtained is shown in Supplementary Figs 4 and 5. The correlation of z-scores (region of interest-wise two-sample t-test) between the two data sets reached 0.85 ($P < 0.0000$). Moreover, most classification accuracies were $>70\%$ when one of the splits was used to identify the significant regions of interest and train the support vector machine classifier, and the other split was used to test the classification accuracy of the trained model. We also compared the difference between data with and without the global signal. The results are shown in Supplementary Fig. 6. We can see that the most significant regions with or without the global signal are quite consistent, although the significant regions were larger in the case with the global signal.

Discussion

This is the first whole-brain voxel pair-wise analysis of the functional connectivity differences between subjects with autism and controls, and the voxel-based results shown in Fig. 2B, Supplementary Fig. 1 and Table 1 are therefore of great interest. Clusters of voxels with altered functional connectivity in autism were associated with the MTG; with the precuneus and paracentral lobule in the parietal cortex; and with the ventromedial prefrontal cortex and other frontal areas. The functional connectivity links between most of these clusters of voxels were decreased (Fig. 3), while the functional connectivity of some of these areas, especially the connectivity of the medial thalamus with the postcentral gyrus and MTG was increased (Fig. 3). The functional significance and correlation with the symptoms of these changes and of the altered functional connectivity between these areas are considered next. In presenting this discussion, we relate the present findings to evidence from other studies to help assess the functional significance of the brain areas in which differences were found in this study between the autistic and typically developing populations, but recognize that correspondences between brain regions identified in different studies do need to be carefully evaluated.

The MTG voxel clusters are in a region that may relate to face processing (in the cortex in the superior temporal sulcus, STS) and to theory of mind impairments in autism. Rolls and colleagues (Perrett *et al.*, 1982; Rolls, 2011) discovered face cells not only in the macaque inferior temporal visual cortex, where they provide transform-invariant representations of face identity (Rolls and Treves, 2011; Rolls, 2012), but also in the cortex in the STS (Baylis *et al.*, 1987; Hasselmo *et al.*, 1989*a*), where the neurons respond to face expression (Hasselmo *et al.*, 1989*a*) and to movements and gestures of the head and body and gaze direction used in social communication (Perrett *et al.*, 1985*a*, *b*; Hasselmo *et al.*, 1989*b*). For example, a neuron might respond to both turning the head away, and to closing the eyes, both of which are signals related to social communication (Hasselmo *et al.*, 1989*b*). Faces including those with expressions activate a region that corresponds in humans, with coordinates that include [−49 −36 2], [−49 −42 4] and [52 −42 4] (Critchley *et al.*, 2000). Now the coordinates of the posteroventral part of the MTG voxels with altered functional connectivity in our investigation were [−56 −37 2], and on this basis is likely to be a face expression processing region. The altered functional connectivity in this area in autism is of great interest, for some of the key typical symptoms of autism spectrum disorder are face processing and especially face expression processing deficits (Lai *et al.*, 2014), which will impair social and emotional communication (Rolls, 2014). Further, in a meta-analysis of functional MRI studies on the cortex in the STS/along the MTG, a posterior cluster of activations was identified with mean [−50 −55 14] that reflected visual motion processing, audio-visual correspondence (e.g. the sound and sight of an utterance), and face processing (Hein and Knight, 2008) (all typical of this region in macaques; Baylis *et al.*, 1987; Hasselmo *et al.*, 1989*a*, *b*; Rolls, 2014). We note that this correspondence is based in our case on a large sample of 927 individuals, and in the data referred to comprised a meta-analysis of many studies (Hein and Knight, 2008), so the data sets are sufficiently large that some reliance on them is reasonable.

The MTG region we identified with altered functional connectivity also has a more antero-dorsal band extending from [−54 −2 −12] anteriorly to [−54 −50 18] posteriorly (Fig. 2). A more anterior cluster of activations in the STS (with mean at [−57 −19 −4]) is related to speech processing in a meta-analysis (Hein and Knight, 2008). In the meta-analysis, activations related to theory of mind were equally distributed over the anterior and posterior clusters (Hein and Knight, 2008). On the right, the MTG/ITG cluster has coordinates [60 −9 −25], and this region is implicated in theory of mind (Hein and Knight, 2008). Thus the region that we identified with reduced functional cortical connectivity in autism spectrum disorder in the MTG/STS has functions related also to theory of mind and even speech processing. This is fascinating, given that there are major impairments of theory of mind

and communication in autism spectrum disorder (Lai *et al.*, 2014).

The details of the changes in the connectivity of the MTG voxels are of interest, and are discussed using the voxel-based voxel connectivity analysis parcellated by AAL regions shown in Fig. 3. The functional connectivity between the medial thalamus (the area shown in Supplementary Fig. 1) and the MTG was increased (Fig. 3). However, in addition to this, it is shown in Fig. 3 that there is reduced functional connectivity of the MTG (and ITG) with the ventromedial prefrontal cortex (ORBsupmed), a region involved in emotion (Rolls, 2014, 2015), including neurons with firing related to face expression (Rolls *et al.*, 2006). Indeed, the cortex in the macaque STS that contains face expression neurons projects to the orbitofrontal cortex in which face expression neurons are also found (Rolls *et al.*, 2006). This is of interest, for the orbitofrontal cortex is important in social behaviour communication (Rolls, 2014), when damaged in humans produces face and voice emotional expression identification impairments (Hornak *et al.*, 1996, 2003), and has connections with the amygdala, which also contains face-selective neurons (Leonard *et al.*, 1985), and both are implicated in autism in some other approaches (Baron-Cohen *et al.*, 1999; Lombardo *et al.*, 2010; Nordahl *et al.*, 2012). Further evidence for the importance of the ventromedial prefrontal cortex in autism is that it is a second main region in which voxels showed reduced functional connectivity (Fig. 2, Supplementary Fig. 2 and Table 1, ORBsupmed), and this reduced connectivity was not only with the MTG and ITG, but also with the precuneus and cuneus (Fig. 3). There is also reduced functional connectivity of the MTG with areas involved in spatial function and the sense of self, including the precuneus and cuneus. We interpret this as showing that there is cortical disconnection of the MTG with other cortical areas implicated in the present analysis as being related to autism, and this disconnection of the MTG region, given the contributions it appears to make to face expression processing and theory of mind, from other cortical areas is, we hypothesize, relevant to how the symptoms of autism arise. In this context, the reduced functional connectivity of the MTG with areas involved in emotion, the ventromedial prefrontal cortex, and areas involved in the sense of self (the precuneus and its connected areas), seems to be relevant to autism spectrum disorder, in which disorders of face processing, emotional and social responses, and theory of mind (to which the sense of self contributes) are important.

The third main set of voxels with reduced functional connectivity is in the precuneus and cuneus region, which is part of medial parietal cortex area 7 (Fig. 2). The precuneus is a region with spatial representations not only of the self, but also of the spatial environment, and it may be partly in relation to this type of representation that damage to this region impairs the sense of self and agency (Cavanna and Trimble, 2006). The reduced functional connectivity of this region is therefore of great interest in relation to the symptoms of autism that relate to not having a theory of others' minds, for which a representation (or 'theory') of oneself in the world may be important (Lombardo *et al.*, 2010). The precuneus has associated with it the adjoining paracentral lobule, which is part of the superior parietal cortex with somatosensory and perhaps visual spatial functions, and has strong anatomical connections with the precuneus (Margulies *et al.*, 2009). Both the paracentral lobule with its body and spatial representation, and the precuneus, operate together to produce a sense of self, in which the representation of the body and how it acts in space is likely to be an important component (Cavanna and Trimble, 2006). We therefore hypothesize that the reduced functional connectivity of these precuneus/superior parietal cortex (paracentral lobule) regions is related to the altered representation or disconnection of the representation of oneself in the world that may contribute to the reduction in the theory of mind in autism (Lombardo *et al.*, 2010). In this context the reduced functional connectivity of this precuneus region with the MTG/ITG/STS areas (Fig. 3) is of interest, for theory of mind including of oneself and others, and face and voice communication with others, would seem to be a set of functions that should normally be usefully communicating to implement social behaviour, which is impaired in autism. The reduced functional connectivity of this paracentral lobule with the somatosensory cortex (PoCG) (Fig. 3) in autism may reflect the fact that somatosensory inputs are likely to be important in the body and self-related functions of the parietal cortex.

The increased functional connectivity between the thalamus and MTG, STG and post-central gyrus found in autism in this analysis was not correlated with the ADOS autism symptom scores (Table 2), and for this reason we do not have a particular interpretation of these changes. We do note that increased functional connectivity between the thalamus and post-central gyrus is found in schizophrenia, and might be related to neurodevelopmental differences (Woodward *et al.*, 2012).

The voxel-based analysis described here was especially important because it provided evidence about exactly where the altered functional connectivity was different in autistic subjects compared to controls. By using voxel-based analysis we were able to show for example that areas in the MTG implicated in processing face expression (Critchley *et al.*, 2000), and also other MTG areas implicated in theory of mind (Hein and Knight, 2008), are both implicated as having altered functional connectivity in autism. The voxel-based analysis also showed that it is a medial/anterior part of the thalamus that has increased connectivity with the MTG, and this part of the thalamus is probably directly connected to temporal cortical areas as shown by diffusion tractography (Johansen-Berg *et al.*, 2005). Further, because voxel clusters may span AAL regions, incorrect inferences may be drawn by the use of AAL parcellation. For example ROIs 19 and 20 in Table 1 are parcellated as MTG and ITG, but are in fact the same cluster of voxels in the right MTG. We suggest that an

important way forward, in view of the usefulness of pair-wise voxel-based analyses that is made evident in this paper, would be to continue with voxel-based analysis, but with even larger samples than the large samples used here, to provide more statistical power, to reveal further clusters of voxels, in for example the amygdala, that are linked to the voxel clusters described in this paper, and to obtain further correlations between functional connectivity and the different symptom scores of people with autism spectrum disorder.

The analysis of the neural basis of autism described here was based on resting state functional connectivity. This complements other approaches such as neuroimaging activation studies by focussing on measures of functional connectivity, and by doing this when no external stimuli are applied, which may enable the inherent functional relations between brain areas to be investigated, as the system may be more largely influenced by statistical fluctuations and noise in the system (Deco *et al.*, 2013*a*, *b*). However, it is not always sufficiently acknowledged that during the resting state in the magnet with the eyes closed or when looking at a fixation point with no other assigned task, one may well be thinking and mentalizing about one's plans for the day, other pending activities etc, which will almost always involve thinking about oneself, and about other people, i.e. other selves. The 'default mode network' may perhaps with this perspective, be thought of as an 'inner mentalizing' network. It may be that this mentalizing process is different in people with autism, who may perform this type of thinking much less, or in a different way (Lai *et al.*, 2014). So we point out that resting state functional MRI in autistic people may help to reveal differences in their brains relative to controls, in part because the thinking of people with autism may be different during resting state functional MRI. Indeed, this difference of thinking during the imaging may contribute to the usefulness of the type of investigation described here of the brain systems implicated in autism.

In conclusion, we have described the first pair-wise voxel-level analysis of functional connectivity in autism, made possible by the great efforts put into acquiring the data in the ABIDE database, which we fully acknowledge and appreciate. We have identified a key system in the MTG/STS sulcus region that has reduced functional connectivity with other cortical areas (and increased connectivity with the medial thalamus), which is implicated in face expression and motion processing involved in social behaviour, and which has onward connections to the orbitofrontal cortex/ventromedial prefrontal cortex. The same system is implicated in theory of mind processing, and in audio-visual integration for e.g. speech, and possibly in further aspects of communication using language. We have identified a second main system with reduced cortical connectivity in autism, the ventromedial prefrontal cortex (ORBsupmed), which itself is implicated in emotion and social communication by virtue of its reward and punishment, including face expression, processing (Rolls, 2014). Its reduced connectivity includes its connectivity with both the MTG regions implicated in face expression and theory of mind processing, and the precuneus/cuneus region (Fig. 3) involved in the sense of self. We have identified a third key system in the precuneus/superior parietal lobule (including paracentral lobule) region with reduced functional connectivity which is implicated in spatial functions including of oneself, and of the spatial environment, and have suggested that this provides an important contribution to theory of mind processing, which is impaired in autism. The hypothesis that we have in mind is that these types of functionality, face expression-related, and of one's self and the environment, are important components of the computations involved in theory of mind, whether of oneself or of others, and that reduced functional connectivity within and between the components of this circuitry may make a major contribution to the symptoms of autism. The reduced functional connectivity could reflect reduced connection strengths within and between areas, or impaired functioning of one of more of the areas that leads to reduced functional connectivity.

Funding

J.F. is a Royal Society Wolfson Research Merit Award holder. The research was partially supported by the National Centre for Mathematics and Interdisciplinary Sciences (NCMIS) of the Chinese Academy of Sciences and Key Program of National Natural Science Foundation of China (No. 91230201); and National High Technology Research and Development Program of China under grant No. 2015AA020507, by grants from the National Natural Science Foundation of China Grant 61271396, 11471081 and 11101429 to W.C. J.Z. is supported by National Science Foundation of China (NSFC 61104143 and 61104224), and special Funds for Major State Basic Research Projects of China (2015CB856003).

Supplementary material

Supplementary material is available at *Brain* online.

References

Assaf M, Jagannathan K, Calhoun VD, Miller L, Stevens MC, Sahl R, et al. Abnormal functional connectivity of default mode sub-networks in autism spectrum disorder patients. Neuroimage 2010; 53: 247–56.

Bach FR, Jordan MI. Kernel independent component analysis. J Mach Learn Res 2003; 3: 1–48.

Baron-Cohen S, Ring HA, Wheelwright S, Bullmore ET, Brammer MJ, Simmons A, et al. Social intelligence in the normal and autistic brain: an fMRI study. Eur J Neurosci 1999; 11: 1891–8.

Baylis GC, Rolls ET, Leonard CM. Functional subdivisions of the temporal lobe neocortex. J Neurosci 1987; 7: 330–42.

Cavanna AE, Trimble MR. The precuneus: a review of its functional anatomy and behavioural correlates. Brain 2006; 129 (Pt 3): 564–83.

Critchley H, Daly E, Phillips M, Brammer M, Bullmore E, Williams S, et al. Explicit and implicit neural mechanisms for processing of social information from facial expressions: a functional magnetic resonance imaging study. Hum Brain Mapp 2000; 9: 93–105.

de Reus MA, Van den Heuvel MP. The parcellation-based connectome: Limitations and extensions. Neuroimage 2013; 80: 397–404.

Deco G, Jirsa VK, McIntosh AR. Resting brains never rest: computational insights into potential cognitive architectures. Trends Neurosci 2013a; 36: 268–74.

Deco G, Ponce-Alvarez A, Mantini D, Romani GL, Hagmann P, Corbetta M. Resting-state functional connectivity emerges from structurally and dynamically shaped slow linear fluctuations. J Neurosci 2013b; 33: 11239–52.

Di Martino A, Yan C, Li Q, Denio E, Castellanos F, Alaerts K, et al. The autism brain imaging data exchange: towards a large-scale evaluation of the intrinsic brain architecture in autism. Mol Psychiatry 2014; 19: 659–67.

Dichter GS, Felder JN, Green SR, Rittenberg AM, Sasson NJ, Bodfish JW. Reward circuitry function in autism spectrum disorders. Soc Cogn Affect Neurosci 2012a; 7: 160–72.

Dichter GS, Richey JA, Rittenberg AM, Sabatino A, Bodfish JW. Reward circuitry function in autism during face anticipation and outcomes. J Autism Dev Disord 2012b; 42: 147–60.

Gotts SJ, Simmons WK, Milbury LA, Wallace GL, Cox RW, Martin A. Fractionation of social brain circuits in autism spectrum disorders. Brain 2012; 135: 2711–25.

Hasselmo ME, Rolls ET, Baylis GC. The role of expression and identity in the face-selective responses of neurons in the temporal visual cortex of the monkey. Behav Brain Res 1989a; 32: 203–18.

Hasselmo ME, Rolls ET, Baylis GC, Nalwa V. Object-centred encoding by face-selective neurons in the cortex in the superior temporal sulcus of the the monkey. Exp Brain Res 1989b; 75: 417–29.

Hein G, Knight RT. Superior temporal sulcus–It's my area: or is it? J Cogn Neurosci 2008; 20: 2125–36.

Hornak J, Bramham J, Rolls ET, Morris RG, O'Doherty J, Bullock PR, et al. Changes in emotion after circumscribed surgical lesions of the orbitofrontal and cingulate cortices. Brain 2003; 126: 1691–712.

Hornak J, Rolls ET, Wade D. Face and voice expression identification in patients with emotional and behavioural changes following ventral frontal lobe damage. Neuropsychologia 1996; 34: 247–61.

Johansen-Berg H, Behrens TE, Sillery E, Ciccarelli O, Thompson AJ, Smith SM, et al. Functional-anatomical validation and individual variation of diffusion tractography-based segmentation of the human thalamus. Cereb Cortex 2005; 15: 31–9.

Kenet T, Orekhova EV, Bharadwaj H, Shetty NR, Israeli E, Lee AK, et al. Disconnectivity of the cortical ocular motor control network in autism spectrum disorders. Neuroimage 2012; 61: 1226–34.

Kennedy DP, Adolphs R. The social brain in psychiatric and neurological disorders. Trends Cogn Sci 2012; 16: 559–72.

Kim YS, Leventhal BL, Koh Y-J, Fombonne E, Laska E, Lim E-C, et al. Prevalence of autism spectrum disorders in a total population sample. Am J Psychiatry 2011; 168: 904–12.

Lai MC, Lombardo MV, Baron-Cohen S. Autism. Lancet 2014; 383: 896–910.

Leonard CM, Rolls ET, Wilson FAW, Baylis GC. Neurons in the amygdala of the monkey with responses selective for faces. Behav Brain Res 1985; 15: 159–76.

Liptak T. On the combination of independent tests. Magyar Tud Akad Mat Kutato Int Kozl 1958; 3: 171–97.

Lombardo MV, Chakrabarti B, Bullmore ET, Sadek SA, Pasco G, Wheelwright SJ, et al. Atypical neural self-representation in autism. Brain 2010; 133: 611–24.

Lynch CJ, Uddin LQ, Supekar K, Khouzam A, Phillips J, Menon V. Default mode network in childhood autism: posteromedial cortex heterogeneity and relationship with social deficits. Biol Psychiatry 2013; 74: 212–9.

Margulies DS, Vincent JL, Kelly C, Lohmann G, Uddin LQ, Biswal BB, et al. Precuneus shares intrinsic functional architecture in humans and monkeys. Proc Natl Acad Sci USA 2009; 106: 20069–74.

Maximo JO, Cadena EJ, Kana RK. The implications of brain connectivity in the neuropsychology of Autism. Neuropsychol Rev 2014; 24: 16–31.

Minshew NJ, Keller TA. The nature of brain dysfunction in autism: functional brain imaging studies. Curr Opin Neurol 2010; 23: 124.

Müller RA, Shih P, Keehn B, Deyoe JR, Leyden KM, Shukla DK. Underconnected, but how? A survey of functional connectivity MRI studies in autism spectrum disorders. Cereb Cortex 2011; 21: 2233–43.

Nordahl CW, Scholz R, Yang X, Buonocore MH, Simon T, Rogers S, et al. Increased rate of amygdala growth in children aged 2 to 4 years with autism spectrum disorders: a longitudinal study. Arch Gen Psychiatry 2012; 69: 53–61.

Perrett DI, Rolls ET, Caan W. Visual neurons responsive to faces in the monkey temporal cortex. Exp Brain Res 1982; 47: 329–42.

Perrett DI, Smith PA, Potter DD, Mistlin AJ, Head AS, Milner AD, et al. Visual cells in the temporal cortex sensitive to face view and gaze direction. Proc R Soc Lond B 1985a; 223: 293–317.

Perrett DI, Smith PAJ, Mistlin AJ, Chitty AJ, Head AS, Potter DD, et al. Visual analysis of body movements by neurons in the temporal cortex of the macaque monkey: a preliminary report. Behav Brain Res 1985b; 16: 153–70.

Power JD, Mitra A, Laumann TO, Snyder AZ, Schlaggar BL, Petersen SE. Methods to detect, characterize, and remove motion artifact in resting state fMRI. Neuroimage 2014; 84: 320–41.

Rolls ET. Face neurons. In: Calder AJ, Rhodes G, Johnson MH, Haxby JV, editors. The Oxford Handbook of Face Perception. Oxford: Oxford University Press; 2011. p. 51–75.

Rolls ET. Invariant visual object and face recognition: neural and computational bases, and a model, VisNet. Front Comput Neurosci 2012; 6, 35: 1–70.

Rolls ET. Emotion and decision-making explained. Oxford: Oxford University Press; 2014.

Rolls ET. Limbic systems for emotion and for memory, but no single limbic system. Cortex 2015; 62: 119–57.

Rolls ET, Critchley HD, Browning AS, Inoue K. Face-selective and auditory neurons in the primate orbitofrontal cortex. Exp Brain Res 2006; 170: 74–87.

Rolls ET, Treves A. The neuronal encoding of information in the brain. Prog Neurobiol 2011; 95: 448–90.

Shih P, Shen M, Öttl B, Keehn B, Gaffrey MS, Müller RA. Atypical network connectivity for imitation in autism spectrum disorder. Neuropsychologia 2010; 48: 2931–9.

Tzourio-Mazoyer N, Landeau B, Papathanassiou D, Crivello F, Etard O, Delcroix N, et al. Automated anatomical labeling of activations in SPM using a macroscopic anatomical parcellation of the MNI MRI single-subject brain. Neuroimage 2002; 15: 273–89.

Uddin LQ, Supekar K, Lynch CJ, Khouzam A, Phillips J, Feinstein C, et al. Salience network–based classification and prediction of symptom severity in children with autism. JAMA Psychiatry 2013; 70: 869–79.

Woodward ND, Karbasforoushan H, Heckers S. Thalamocortical dysconnectivity in schizophrenia. Am J Psychiatry 2012; 169: 1092–9.

Supplementary Material

Autism: Reduced Functional Connectivity between Cortical Areas Involved in Face Expression, Theory of Mind, and the Sense of Self

Wei Cheng[1, #] Edmund T. Rolls[2,3, #] Huaging Gu[4,*] Jie Zhang[1] Jianfeng Feng[1, 2]

1. Centre for Computational Systems Biology, Fudan University, Shanghai, PR China
2. University of Warwick, Department of Computer Science, Coventry CV4 7AL, UK
3. Oxford Centre for Computational Neuroscience, Oxford, UK
4. School of Aerospace Engineering and Applied Mechanics, Tongji University, Shanghai 200092, PR China

Table S1. The demographic and clinical characteristics of participants satisfying inclusion criteria.

Variables	Number of sites	Number of subjects	Control			Autism			Group comparisons	
			Sub n	Mean	SD	Sub n	Mean	SD	Statistic	p value
AGE_AT_SCAN	16	927	509	16.4	7.08	418	17.17	7.97	-1.55	0.12
FIQ	16	856	471	110.62	11.93	385	105.7	14.16	5.44	<0.001
VIQ	12	789	428	111.10	12.84	361	104.5	15.87	6.43	<0.001
PIQ	13	787	425	107.24	12.56	362	105.3	15.17	1.89	0.058
ADOS_TOTAL	13	323	30	1.30	1.393	293	11.64	3.761	/	/
ADOS_COMM	12	301	30	0.533	0.681	271	3.771	1.507	/	/
ADOS_SOCIAL	12	301	30	0.766	0.971	271	7.952	2.751	/	/
ADOS_STEREO_BEHAV	8	264	30	0.066	0.253	234	1.995	1.532	/	/
ADI_R_SOCIAL_TOTAL_A	13	285	/	/	/	285	19.84	5.620	/	/
ADI_R_VERBAL_TOTAL_BV	13	286	/	/	/	286	15.82	4.618	/	/
ADI_RRB_TOTAL_C	13	285	/	/	/	285	6.119	2.586	/	/
ADI_R_ONSET_TOTAL_D	11	220	/	/	/	220	3.195	1.272	/	/
Sex (male/female)	16	927	424/85	/	/	367/51	/	/	3.71	0.0541
Handedness (right/others)	16	927	458/51	/	/	359/59	/	/	3.68	0.055
EYE_STATUS_AT_SCAN (open/ closed)	16	927	369/140	/	/	306/112	/	/	0.058	0.808
DSM_IV_TR (autism/others)	14	384	/	/	/	279/105	/	/	/	/
MEDICATION (yes/no)	12	293	/	/	/	99/194	/	/	/	/

Number of sites: The number of sites including the Variables
Number of subjects: The number of subjects including the Variables
Sub n: The number of subjects including the Variables in controls or in the autistic group
AGE_AT_SCAN: Age at time of scan in years
FIQ: Full IQ
VIQ: Verbal IQ
PIQ: Performance IQ
ADOS_TOTAL: Classic Total Autism Diagnostic Observation Schedule (ADOS) Score
ADOS_COMM: Communication Total Subscore of the Classic ADOS
ADOS_SOCIAL: Social Total Subscore of the Classic ADOS
ADOS_STEREO_BEHAV: Stereotyped Behaviors and Restricted Interests Total Subscore of the Classic ADOS
ADI_R_SOCIAL_TOTAL_A: Reciprocal Social Interaction Subscore (A) Total for Autism Diagnostic Interview-Revised (ADI-R)
ADI_R_VERBAL_TOTAL_BV: Abnormalities in Communication Subscore (B) Total for ADI-R
ADI_RRB_TOTAL_C: Restricted, Repetitive, and Stereotyped Patterns of Behavior Subscore (C) Total for ADI-R
ADI_R_ONSET_TOTAL_D: Abnormality of Development Evident at or Before 36 Months Subscore (D) Total for ADI-R
EYE_STATUS_AT_SCAN: Eye Status During Rest Scan
DSM_IV_TR: DSM_IV_TR Diagnostic Category
MEDICATION: Information on use of medications within the month prior to the scan

Table S2. The names and abbreviations of the regions of interest (ROIs)

NO.	Regions	Abbr.	NO.	Regions	Abbr.
1, 2	Precentral gyrus	PreCG	47, 48	Lingual gyrus	LING
3, 4	Superior frontal gyrus, dorsolateral	SFGdor	49, 50	Superior occipital gyrus	SOG
5, 6	Orbitofrontal cortex, superior part	ORBsup	51, 52	Middle occipital gyrus	MOG
7, 8	Middle frontal gyrus	MFG	53, 54	Inferior occipital gyrus	IOG
9, 10	Orbitofrontal cortex, middle part	ORBmid	55, 56	Fusiform gyrus	FFG
11, 12	Inferior frontal gyrus, opercular part	IFGoperc	57, 58	Postcentral gyrus	PoCG
13, 14	Inferior frontal gyrus, triangular part	IFGtriang	59, 60	Superior parietal gyrus	SPG
15, 16	Orbitofrontal cortex, inferior part	ORBinf	61, 62	Inferior parietal	IPL
17, 18	Rolandic operculum	ROL	63, 64	Supramarginal gyrus	SMG
19, 20	Supplementary motor area	SMA	65, 66	Angular gyrus	ANG
21, 22	Olfactory cortex	OLF	67, 68	Precuneus	PCUN
23, 24	Superior frontal gyrus, medial	SFGmed	69, 70	Paracentral lobule	PCL
25, 26	Orbitofrontal cortex, superior medial	ORBsupmed	71, 72	Caudate nucleus	CAU
27, 28	Gyrus rectus	REC	73, 74	Lenticular nucleus, putamen	PUT
29, 30	Insula	INS	75, 76	Lenticular nucleus, pallidum	PAL
31, 32	Anterior cingulate & paracingulate gyri	ACG	77, 78	Thalamus	THA
33, 34	Cingulate & paracingulate gyri	DCG	79, 80	Heschl gyrus	HES
35, 36	Posterior cingulate gyrus	PCG	81, 82	Superior temporal gyrus	STG
37, 38	Hippocampus	HIP	83, 84	Temporal pole: superior	TPOsup
39, 40	Parahippocampal gyrus	PHG	85, 86	Middle temporal gyrus	MTG
41, 42	Amygdala	AMYG	87, 88	Temporal pole: middle	TPOmid
43, 44	Calcarine fissure & surrounding cortex	CAL	89, 90	Inferior temporal gyrus	ITG
45, 46	Cuneus	CUN			

Table S3. The result of classification based on the voxel-based ROI-wise analysis.

Sites	Sensitivity	Specificity	Accuracy
Caltech	84.21	89.47	86.84
KKI	56.25	87.09	76.59
Leuven	41.37	100.00	73.01
MaxMun	100.00	75.00	92.30
NYU	69.56	87.50	80.00
OHSU	90.90	100.00	96.15
Olin	82.35	87.50	84.84
Pitt	64.28	88.88	76.36
SBL	93.33	66.66	80.00
SDSU	81.81	95.45	90.90
Stanford	100.00	94.44	95.00
Trinity	77.27	79.16	78.26
UCLA	68.29	82.22	75.58
UM	71.42	80.51	76.69
USM	90.38	67.50	80.43
Yale	85.71	80.76	82.97

Table S4. Significant regions of interest (ROIs) identified by the first and second dataset in the voxel-based whole brain analysis. We highlighted regions that exhibit abnormalities in three different cases: whole dataset, the first half and the second half.

ROIs identified by the first split half data							ROIs identified by the second split half data						
No.	**Areas**	**Cluster size #Voxels**	**Peak MA value**	**Peak MNI coordinates**			**No.**	**Areas**	**Cluster size #Voxels**	**Peak MA value**	**Peak MNI coordinates**		
ROI 1	PreCG.L	39	-195	-45	-15	57	**ROI 1**	**PreCG.R**	**29**	**108**	**33**	**-18**	**54**
ROI 2	**PreCG.R**	**164**	**-245**	**36**	**-24**	**54**	**ROI 2**	**SFGdor.L**	**108**	**637**	**-18**	**27**	**45**
ROI 3	**SFGdor.L**	**28**	**231**	**-21**	**27**	**42**	ROI 3	SFGdor.R	73	-986	24	33	57
ROI 4	**MFG.L**	**88**	**-307**	**-39**	**45**	**24**	**ROI 4**	**MFG.L**	**154**	**382**	**-39**	**45**	**24**
ROI 5	**MFG.R**	**30**	**-482**	**51**	**48**	**3**	**ROI 5**	**MFG.R**	**157**	**-376**	**51**	**48**	**3**
ROI 6	IFGoperc.R	70	-112	54	18	21	ROI 6	IFGtriang.L	74	311	-45	42	9
ROI 7	IFGtriang.R	142	-470	51	45	3	ROI 7	IFGtriang.R	53	-288	51	45	6
ROI 8	ROL.R	22	93	66	-6	12	**ROI 8**	**SMA.R**	**26**	**160**	**6**	**-24**	**54**
ROI 9	SMA.L	44	-169	0	18	45	ROI 9	SFGmed.L	51	-225	0	66	3
ROI 10	**SMA.R**	**125**	**201**	**9**	**-21**	**72**	ROI 10	SFGmed.R	90	-296	3	63	3
ROI 11	**ORBsupmed.L**	**26**	**-268**	**0**	**63**	**-3**	**ROI 11**	**ORBsupmed.L**	**80**	**-460**	**0**	**66**	**-3**
ROI 12	**ORBsupmed.R**	**97**	**-433**	**3**	**60**	**-3**	**ROI 12**	**ORBsupmed.R**	**128**	**-530**	**3**	**66**	**-3**
ROI 13	REC.L	31	-143	0	51	-18	ROI 13	REC.L	37	-203	-3	51	-15
ROI 14	REC.R	23	260	6	57	-15	ROI 14	INS.R	31	159	45	18	-9
ROI 15	INS.L	102	-140	-39	3	0	ROI 15	ACG.L	177	-361	-6	42	6
ROI 16	INS.R	65	-102	45	15	-9	ROI 16	ACG.R	124	-186	3	42	3
ROI 17	DCG.L	74	470	0	-39	48	ROI 17	PHG.L	27	-246	-27	-30	-15
ROI 18	DCG.R	129	-330	3	15	42	**ROI 18**	**PoCG.L**	**45**	**-205**	**-54**	**-18**	**51**
ROI 19	CAL.L	58	-421	-9	-63	21	**ROI 19**	**PoCG.R**	**43**	**105**	**39**	**-21**	**48**
ROI 20	**CUN.L**	**64**	**-532**	**-9**	**-66**	**24**	ROI 20	IPL.L	28	-171	-57	-36	54
ROI 21	CUN.R	40	167	18	-78	27	ROI 21	SMG.R	105	-168	57	-36	45
ROI 22	LING.L	21	123	-9	-48	3	**ROI 22**	**PCUN.L**	**57**	**-139**	**-9**	**-57**	**27**
ROI 23	SOG.R	87	163	18	-81	30	**ROI 23**	**PCUN.R**	**64**	**-149**	**6**	**-54**	**24**
ROI 24	MOG.L	55	72	-27	-87	18	ROI 24	CAU.L	37	434	-12	-6	18
ROI 25	MOG.R	28	99	30	-81	27	**ROI 25**	**CAU.R**	**24**	**243**	**15**	**-15**	**21**
ROI 26	IOG.L	21	-89	-21	-90	-9	ROI 26	PUT.L	55	-260	-21	3	-6
ROI 27	**PoCG.L**	**415**	**-1065**	**-54**	**-15**	**48**	ROI 27	PUT.R	39	-152	24	9	3
ROI 28	**PoCG.R**	**380**	**-498**	**39**	**-27**	**54**	ROI 28	PAL.L	23	-241	-21	6	-3
ROI 29	IPL.L	46	-336	-51	-18	39	ROI 29	PAL.R	27	-93	21	6	3
ROI 30	SMG.R	49	262	60	-36	42	**ROI 30**	**THA.L**	**154**	**368**	**-9**	**-9**	**15**
ROI 31	**PCUN.L**	**225**	**-302**	**-9**	**-48**	**9**	**ROI 31**	**THA.R**	**188**	**322**	**15**	**-12**	**18**
ROI 32	**PCUN.R**	**173**	**-362**	**6**	**-51**	**27**	**ROI 32**	**STG.L**	**101**	**147**	**-54**	**-24**	**3**
ROI 33	**PCL.L**	**124**	**-198**	**0**	**-24**	**54**	**ROI 33**	**MTG.L**	**129**	**136**	**-54**	**-27**	**3**
ROI 34	PCL.R	77	175	12	-24	72	**ROI 34**	**MTG.R**	**37**	**-263**	**60**	**0**	**-30**
ROI 35	**CAU.R**	**52**	**761**	**15**	**-6**	**18**	ROI 35	ITG.L	41	-400	-57	-6	-30
ROI 36	**THA.L**	**182**	**514**	**-6**	**-18**	**12**	**ROI 36**	**ITG.R**	**91**	**-305**	**48**	**-6**	**-36**
ROI 37	**THA.R**	**173**	**874**	**12**	**-6**	**12**							
ROI 38	**STG.L**	**84**	**291**	**-54**	**6**	**-12**							
ROI 39	STG.R	137	-238	51	-39	12							
ROI 40	TPOsup.L	35	-296	-54	9	-15							
ROI 41	TPOsup.R	65	505	51	9	-6							

ROI 42	**MTG.L**	**252**	**261**	**-63**	**-21**	**0**	
ROI 43	**MTG.R**	**102**	**-609**	**54**	**-3**	**-27**	
ROI 44	TPOmid.L	21	146	-48	15	-30	
ROI 45	**ITG.R**	**76**	**257**	**60**	**-6**	**-30**	

Figure S1. Location of the altered functional network of the voxel-level whole brain association study. The left side of the brain is on the right of each coronal slice. Voxels with overall increased connectivity are in red, and with reduced connectivity in blue.

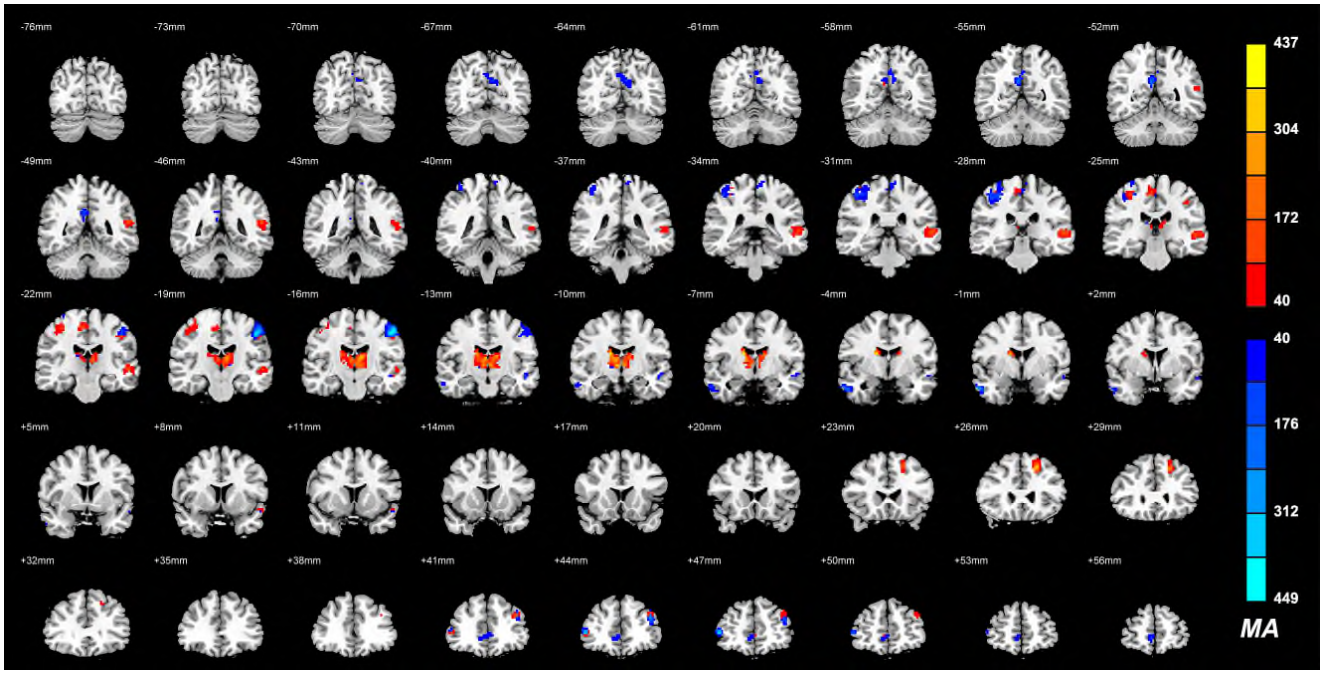

Figure S2. Voxels with different functional connectivity in autism (Bonferroni correction, in this case the effect of IQ was not regressed). **A.** Manhattan plot showing the probability values for each link being different in the autistic group compared to the control group. Each dot is a functional connectivity link between two voxels. Note there are a total of $47636 \times 47635 / 2$ links, and we only plot a dot if $p<10^{-5}$. The red dotted line is the Bonferroni correction threshold 4.4×10^{-11}. The regions indicate the AAL areas in which the voxels were located, with the numbers for each region specified in Table S2. **B.** Location of the voxels that had significantly different altered functional connectivity with other voxels (using whole brain Bonferroni correction). The color bar represents the measure of association (MA, see text) given by the number of significantly affected links relating to each voxel. Voxels that had functional connectivities in the autism population that were weaker than in controls are shown in blue, and that had stronger functional connectivity in the autism population are shown in red. Five main groups of voxels are evident, in the middle temporal gyrus (MTG), ventromedial prefrontal cortex (ORBsupmed), precuneus (PCUN) and paracentral lobule (PCL), the post- and pre-central cortex (PoCG and PreCG), and a medial region of the thalamus (THA). SFGmed - superior frontal gyrus, medial part.

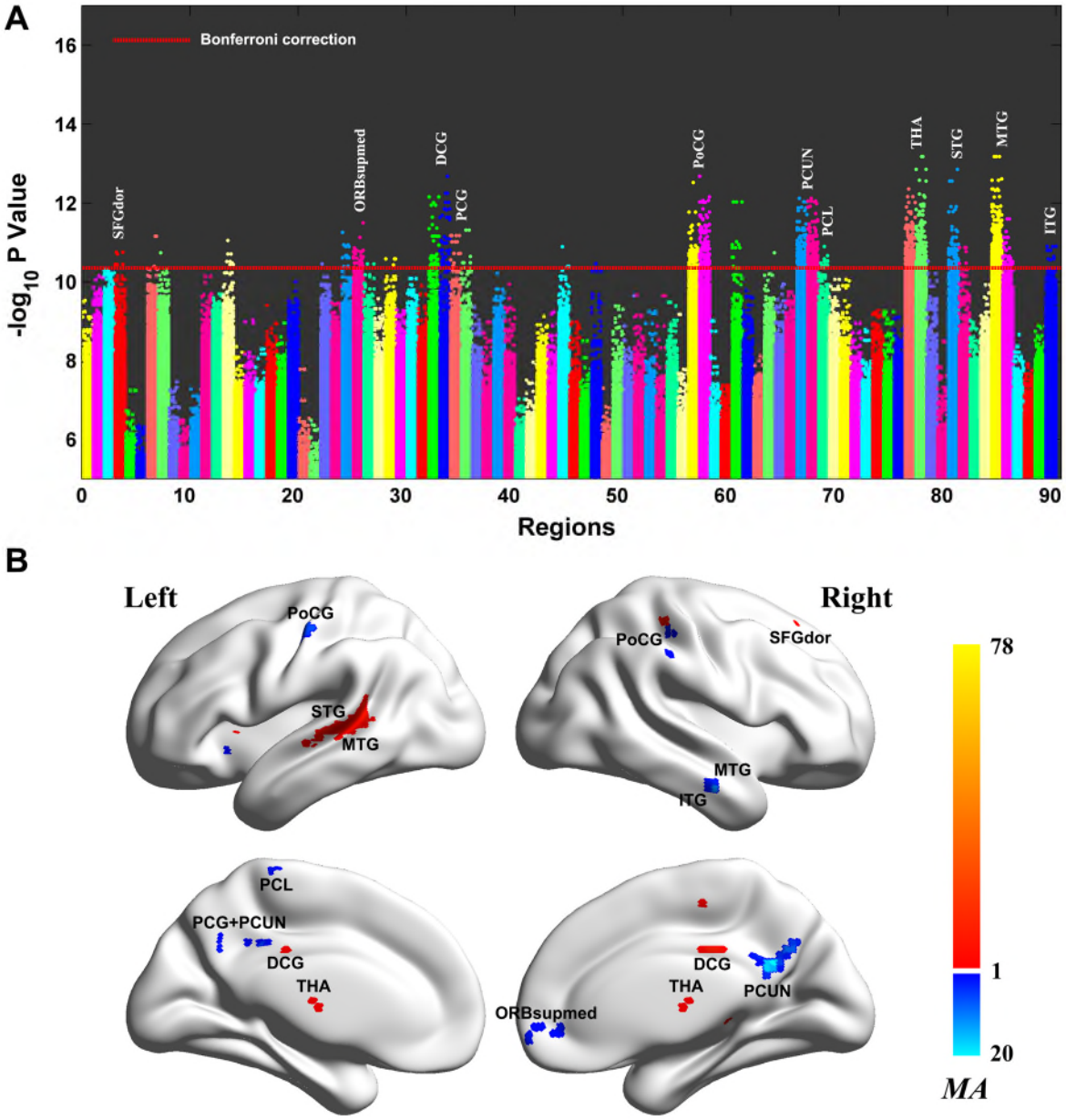

Figure S3. The locations of all voxels in the brain that have significantly different functional connectivities between the autistic and the control population for both datasets (FDR correction, 0.05, *MA* >40, cluster size >30 voxels for the first half and the second half dataset). We highlighted regions that exhibit abnormalities in three different cases: whole dataset, the first half and the second half.

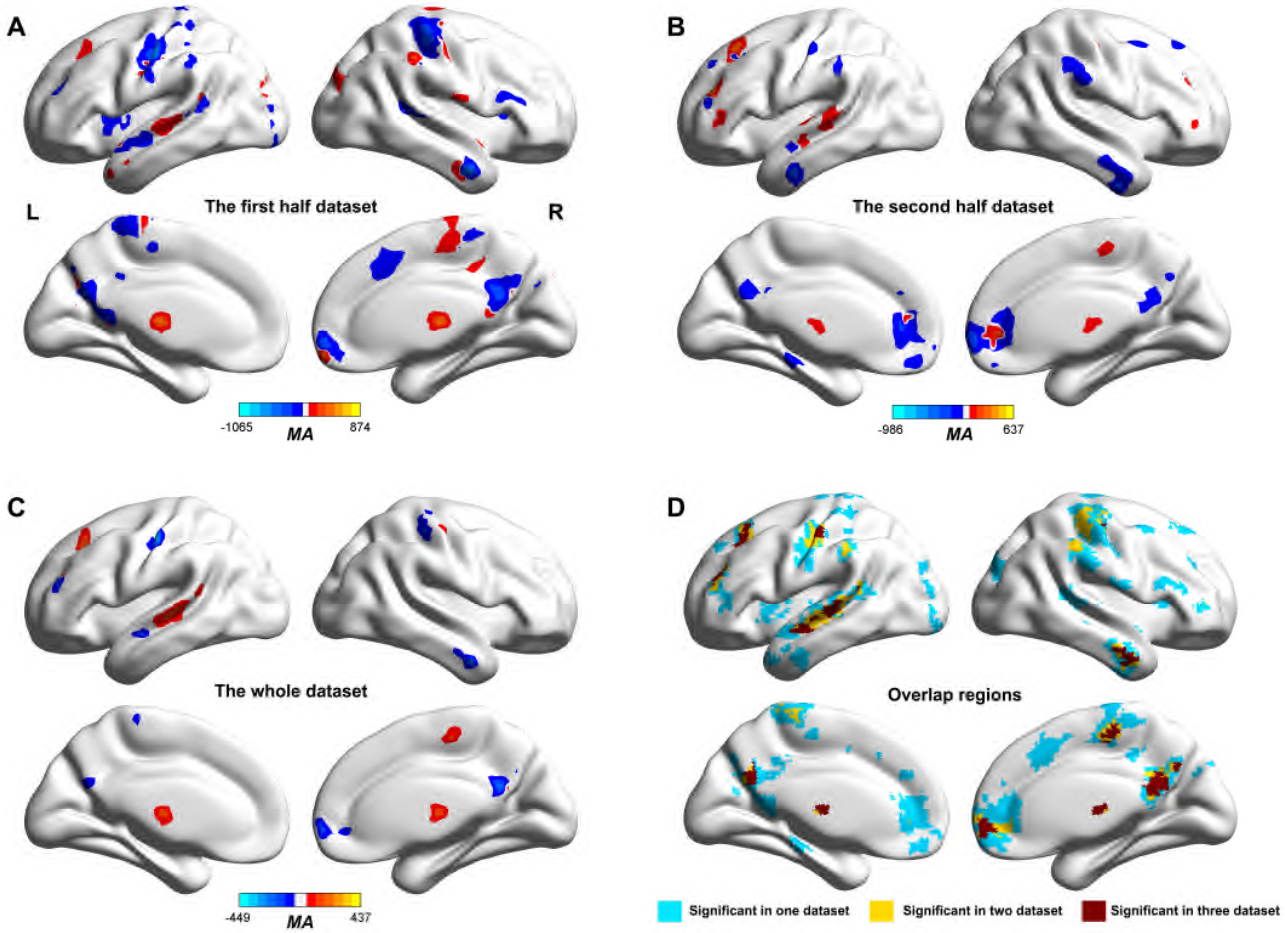

Figure S4. The robustness of ROI-wise analysis. A) The pattern of altered functional connectivity of the first half dataset. The functional connectivity matrix calculated from the BOLD signals in ROIs identified by the first half dataset. B) The pattern of altered functional connectivity of the second half dataset based on the ROIs identified by the first half dataset. C) The correlation of statistics (ROI-wise two-sample t test) between the two datasets. Although the ROIs were defined by the first half dataset, the functional connectivity among those ROIs was also significantly different between the autistic and control populations in the second half dataset in a very similar manner. D, E, F) A similar result to that above. When we used the second half dataset to find the significant ROIs, the first dataset also show similar changed patterns.

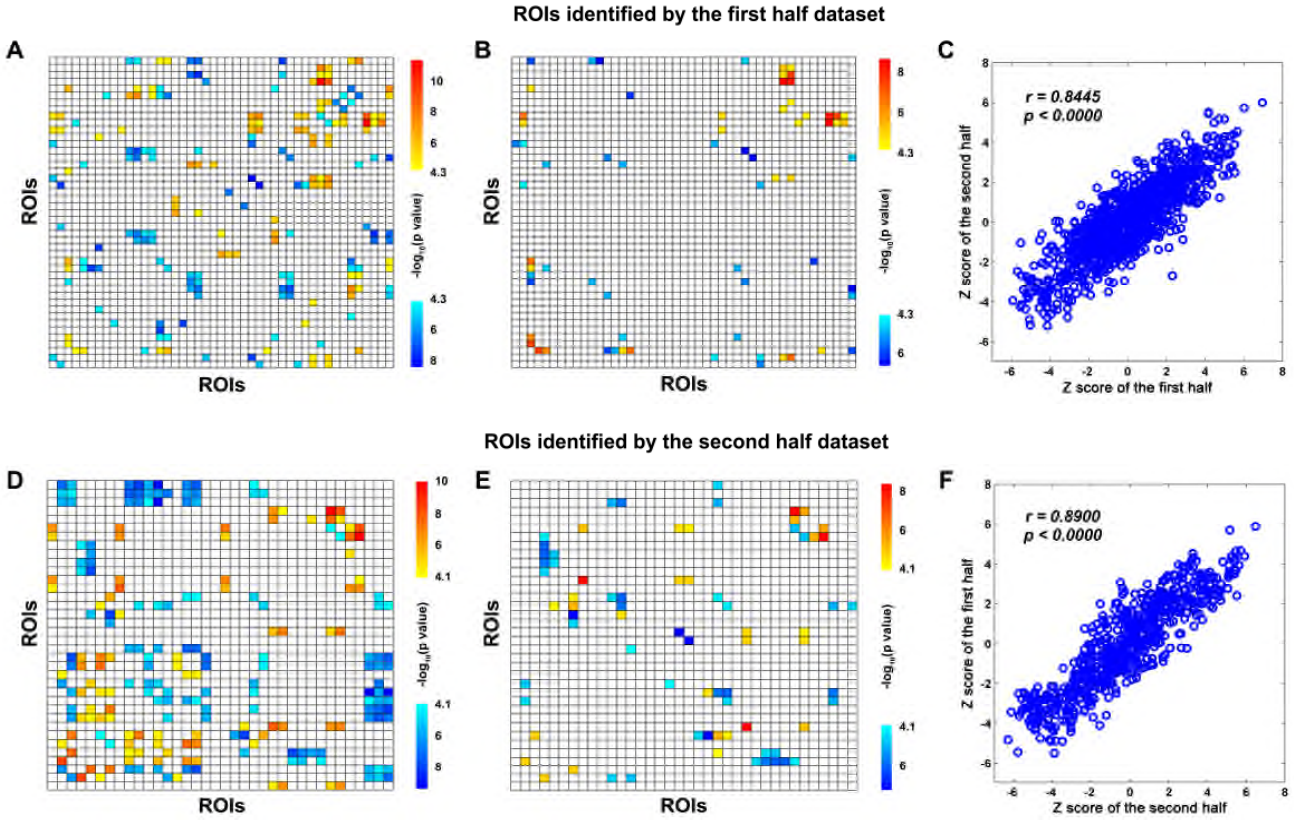

Figure S5. The robustness of classification. A) The first dataset was used to identify the significant ROIs and train the SVM classifier, then the second dataset was used to test classification accuracy of the trained model. B) The second dataset was used to identify the significant ROIs and train the SVM classifier, then the first dataset was used to test classification accuracy of the trained model.

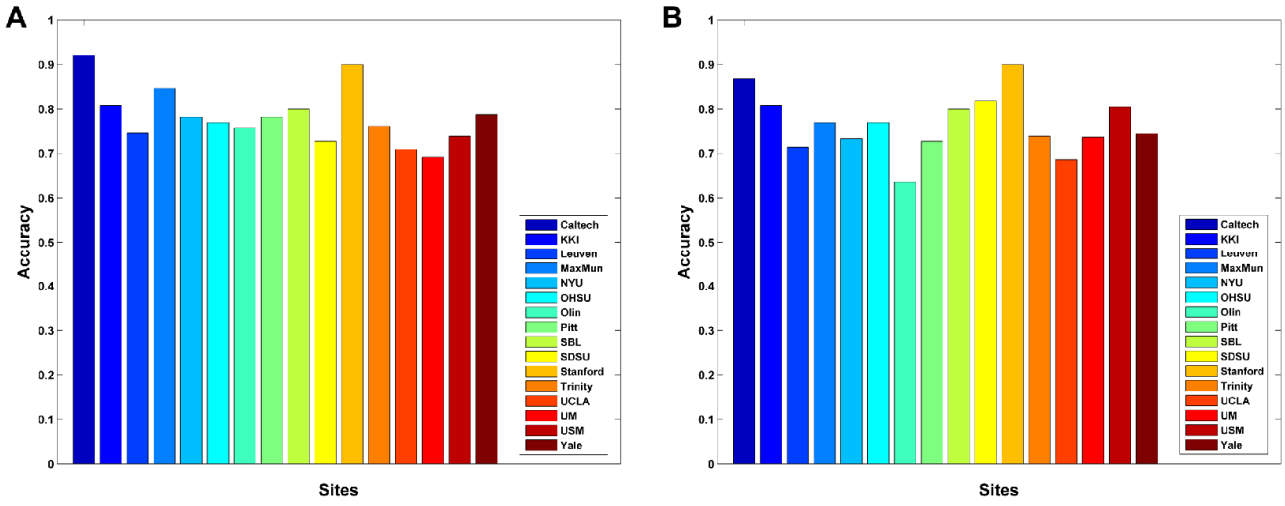

Figure S6. Comparison between the results with (A) and without (B) the global signal.

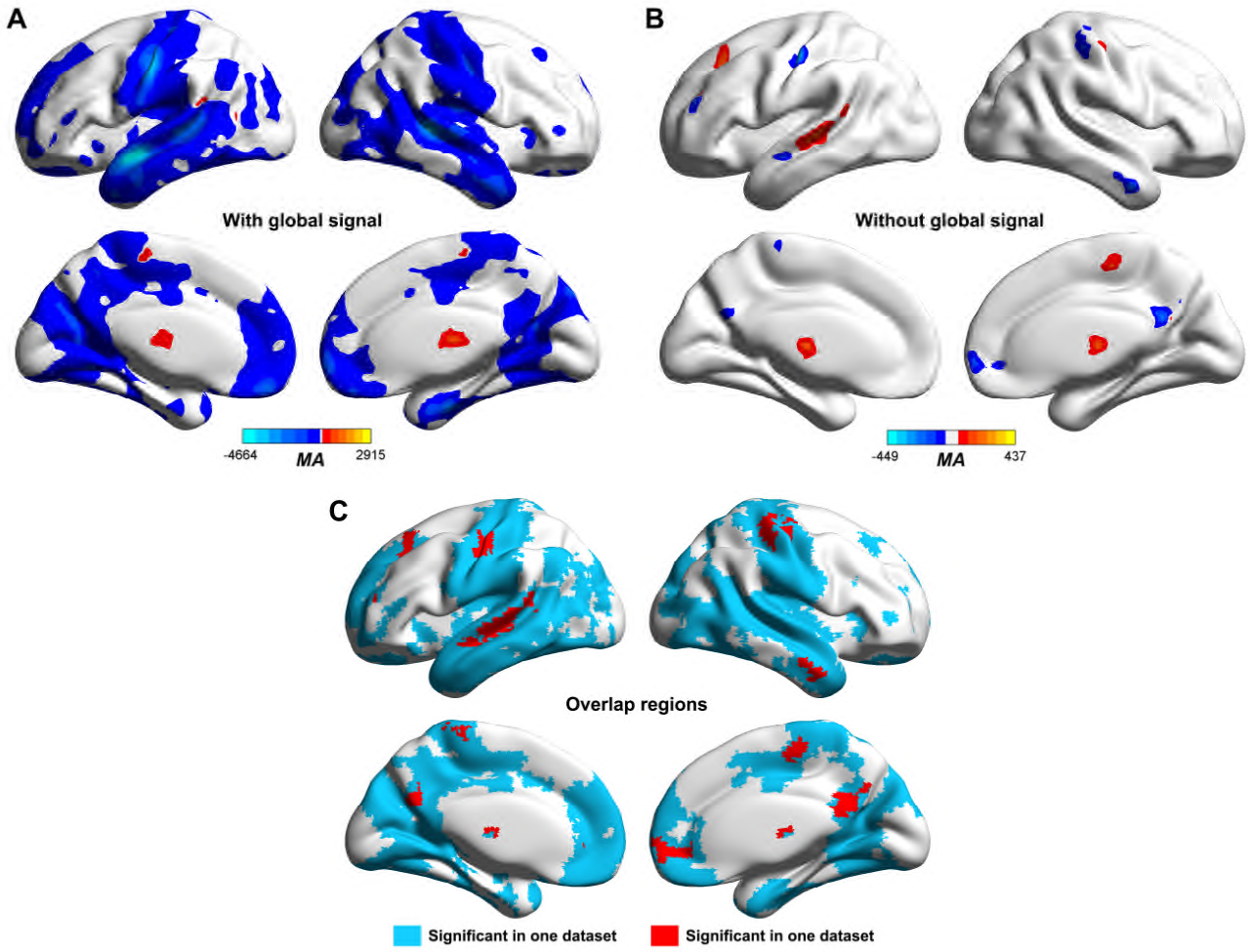

Figure S7. Forest plots showing a meta-analysis of the association of the significant functional connectivities (top 15 links) with autism. We can see that the altered patterns of functional connections were consistent across the datasets from the 16 different imaging centers.

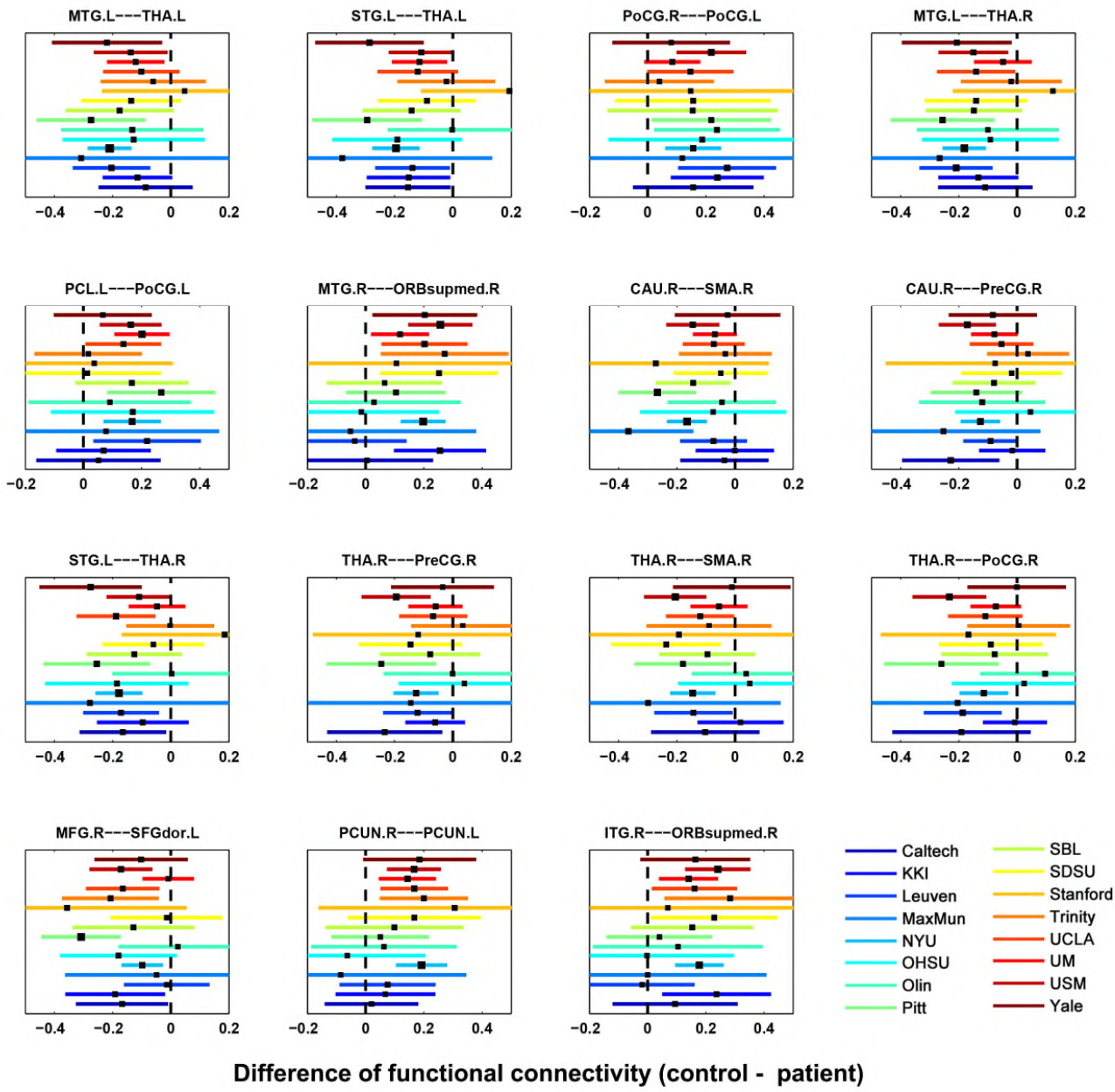

Figure S8. The pair-wise voxel-level functional connectivity that was different between the autistic group and the control group. Each connecting line is a link between two voxels that was different in the autistic and control group. The colors are chosen to be different for links between the different AAL regions. The abbreviations for each brain region are in Table S2.